

# Exactly solvable 1D model explains the low-energy vibrational level structure of protonated methane

Jonathan I. Rawlinson <sup>\*1</sup>, Csaba Fábri<sup>2,3</sup>, and Attila G. Császár<sup>2,3</sup>

<sup>1</sup>School of Mathematics, University of Bristol, Bristol, UK

<sup>2</sup>Laboratory of Molecular Structure and Dynamics, Institute of Chemistry, Eötvös Loránd University, Pázmány Péter sétány 1/A, H-1117 Budapest, Hungary

<sup>3</sup>MTA-ELTE Complex Chemical Systems Research Group, P.O. Box 32, H-1518 Budapest 112, Hungary

March 30, 2021

## Abstract

A new one-dimensional model is proposed for the low-energy vibrational quantum dynamics of  $\text{CH}_5^+$  based on the motion of an effective particle confined to a 60-vertex graph  $\Gamma_{60}$  with a single edge length parameter. Within this model, the quantum states of  $\text{CH}_5^+$  are obtained in analytic form and are related to combinatorial properties of  $\Gamma_{60}$ . The bipartite structure of  $\Gamma_{60}$  gives a simple explanation for curious symmetries observed in numerically exact variational calculations on  $\text{CH}_5^+$

Protonated methane,  $\text{CH}_5^+$ , also called methonium, is considered to be the prototype of pentacoordinated nonclassical carbonium ions [1–3]. The curious carbonium cations yielded an extremely rich chemistry and a Nobel-prize to their discoverer, George Olah [4]. Nevertheless, these are not the only sources of fame for carbonium ions and in particular for  $\text{CH}_5^+$ . Over the last two decades [5], the internal motion of  $\text{CH}_5^+$  has been posing a formidable challenge to high-resolution spectroscopists [5–15]. The most outstanding issue is that the observed spectra of  $\text{CH}_5^+$  remain exceptionally complex even when they are observed at temperatures of a few K [9, 13], due to the quasistructural nature [16] of this molecular ion.

As to the utilization of quantum chemistry to solve the experimental puzzle, through huge numerical efforts accurate rovibrational energy levels and eigenstates have been made available for  $\text{CH}_5^+$  in recent years [7, 12, 14]. These studies have revealed close-lying clusters in the rovibrational energy levels, with fascinating symmetry characteristics. These features have defied explanation by conventional means, motivating the development of novel models for  $\text{CH}_5^+$ . The most important models put forward so far are as follows: (a) particle-on-a-sphere

---

\*jonathanianrawlinson@gmail.com

(POS) [17–23], (b) five-dimensional (5D) rotor (superrotor) [24–26], and (c) quantum graph [15, 27]. So far, the quantum-graph model seems to have resulted in the most satisfactory explanation of the low-energy quantum dynamics of  $\text{CH}_5^+$ , including both vibrations [15] and rotations [27].

Quantum graphs have a long history in chemistry and physics, dating back to Linus Pauling’s description of electrons in organic molecules in the 1930s [28]. They have only recently been introduced to the study of nuclear dynamics, where they have proved useful in high-resolution spectroscopy [15, 27] and also in explaining  $\alpha$ -cluster dynamics in nuclear physics [29, 30]. Quantum graphs [31] are metric graphs, that is each of their edges possesses a length. In the context of rovibrational dynamics of molecules, each vertex of the graph represents a version [32] of an equilibrium structure. Depending on the nuclear permutation-inversion symmetry [32] of the molecule of a given composition, even if the molecule has a single minimum on a given potential energy surface it may possess a large number of versions. The vertices defined by the versions are connected by edges which represent collective internal motions converting different versions into each other. Once a quantum graph is set up, one constructs the one-dimensional (1D) Schrödinger equation for a particle confined to the graph and solves it to determine the energy levels and eigenstates†. In this way, the complex multidimensional rovibrational quantum dynamics of a polyatomic molecule is mapped onto the effective motion of a 1D particle confined to a much simpler space.

In the case of  $\text{CH}_5^+$ , the equilibrium structure, the only one found on its ground electronic state, is composed of a  $\text{H}_2$  unit sitting on top of a  $\text{CH}_3^+$  tripod, an arrangement with  $C_s$  point-group symmetry. The five protons can be rearranged in  $5!=120$  ways, generating 120 symmetry-equivalent versions. These versions become the 120 vertices of a quantum graph  $\Gamma_{120}$  [15]. There are two types of motion interconverting the 120 equivalent versions, equivalent to scrambling the H atoms of  $\text{CH}_5^+$ : the internal rotations of the  $\text{H}_2$  unit by  $60^\circ$  (both clockwise and counterclockwise), and the flip motion that exchanges a pair of protons between the  $\text{H}_2$  and  $\text{CH}_3^+$  units. The barriers to these motions on the potential energy hypersurface of  $\text{CH}_5^+$  [33] are known to be relatively low. It is plausible that the low-energy dynamics is dominated by motion along these particular paths, so that motions other than the internal rotation and flip motions can be disregarded. Thus, one can take these motions to correspond to the edges of  $\Gamma_{120}$ . As one flip edge and two internal rotation edges are connected to each vertex of  $\Gamma_{120}$ , each vertex has a degree of three ( $\Gamma_{120}$  is a 3-regular graph). Due to the nature of the underlying internal motions, the 120 internal rotation and 60 flip edges are assigned effective lengths  $L_{\text{rot}}$  and  $L_{\text{flip}}$ , respectively.

As shown before [15, 27], the quantum graph  $\Gamma_{120}$  reproduces the low-energy rovibrational energy levels of  $\text{CH}_5^+$ , as well as of  $\text{CD}_5^+$ , remarkably well when optimized values of  $L_{\text{flip}}$  and  $L_{\text{rot}}$  are used †. For instance, the  $\Gamma_{120}$  model perfectly reproduces the curious block structure (states occurring in groups of 15 and 30, see Table 1) of the vibrational eigenstates of  $\text{CH}_5^+$ , first noted in a variational study of Wang and Carrington [12] and later confirmed in Ref. 14. As seen in Table 1, rovibrational eigenstates of  $\text{CH}_5^+$  are labelled by irreducible representations (irreps) of the molecular symmetry (MS) group [32]  $S_5^* = S_5 \times \{E, E^*\}$ , generated by  $S_5$  permutations of the five protons together with spatial inversion  $E^*$  ( $E$  denotes the identity operation).

Beyond the existence of blocks, in Table 1 one can notice other clear symmetry relations for the first 60 quantum states. A comparison of the group-theoretic relation

$$(A_1^+ \oplus G_1^+ \oplus H_1^+ \oplus H_2^+) \otimes A_2^- \simeq A_2^- \oplus G_2^- \oplus H_2^- \oplus H_1^- \quad (1)$$

Block 1	Block 2
0 – 60 cm <sup>-1</sup> (15,15)	110 – 200 cm <sup>-1</sup> (15,15)
$A_1^+ \oplus G_1^+ \oplus H_1^+ \oplus H_2^+ \oplus$	$G_1^+ \oplus H_1^+ \oplus I^+ \oplus$
$G_2^- \oplus H_2^- \oplus I^-$	$A_2^- \oplus G_2^- \oplus H_1^- \oplus H_2^-$

Table 1: The block structure characterizing the first 60 vibrational states of CH<sub>5</sub><sup>+</sup>, revealed in variational computations [12, 14]. The numbers in parentheses give the total number of positive and negative parity states within a block, reflecting the degeneracy of the states

with the data in Table 1 suggests a direct correspondence between the 15 positive-parity states in Block 1 [appearing on the left-hand side (LHS) of Eq. (1)] and the 15 negative-parity states in Block 2 [right-hand side (RHS) of Eq. (1)]. Likewise,

$$(G_2^- \oplus H_2^- \oplus I^-) \otimes A_2^- \simeq G_1^+ \oplus H_1^+ \oplus I^+, \quad (2)$$

suggesting a link between the 15 negative-parity states in Block 1 and the positive-parity states in Block 2. These remarkable symmetry relations have been lacking any simple explanation, even in terms of the  $\Gamma_{120}$  model. As this paper proves, introduction of the simplest quantum-graph model,  $\Gamma_{60}$ , of the quantum dynamics of CH<sub>5</sub><sup>+</sup>, derived from  $\Gamma_{120}$ , is sufficient to explain the curious energy-level and symmetry structure of the lowest vibrational states of CH<sub>5</sub><sup>+</sup>, and, as a bonus feature, it allows the analytic determination of the quantum states of the model problem.

Let us start our journey toward the simplest model with the quantum graph  $\Gamma_{120}$ . We recall two important characteristics of our original study [15]. First, we neglect the potential energy along the edges of  $\Gamma_{120}$ , since the barriers to the internal rotation and flip motions are small (about 30 cm<sup>-1</sup> and 300 cm<sup>-1</sup>, respectively [33]). Second, we fix the effective edge lengths  $L_{\text{flip}}$  and  $L_{\text{rot}}$ . In Ref. 15 this was done by an optimization procedure to give the best fit to either 7D or 12D reference data. In both cases the optimized  $L_{\text{flip}}$  was much smaller than the optimized  $L_{\text{rot}}$ , with the ratio  $L_{\text{flip}}/L_{\text{rot}} = 1.0/61.2$  in the 7D case.

Our new model is based on the following idea: the ratio  $L_{\text{flip}}/L_{\text{rot}}$  is so small that it is tempting to imagine shrinking the flip edges to zero length, identifying the two vertices at the endpoints of each flip edge to give a single vertex. Setting  $L_{\text{flip}} = 0$  has a negligible effect on the accuracy of the fit, at least at low energies. At the same time, this approximation gives a huge simplification: the number of vertices is halved and we get a new quantum graph,  $\Gamma_{60}$ , with only the internal rotation edges remaining. It is reasonable to identify each new vertex with the midpoint of the (now contracted) flip edge, which is a  $C_{2v}$ -symmetric transition state, as illustrated in Fig. 1.  $\Gamma_{60}$  represents 60 symmetry-equivalent versions of this configuration. We propose that the most important characteristics of the low-energy quantum states of CH<sub>5</sub><sup>+</sup> can be understood in terms of a 1D, potential-free motion between these versions corresponding to the vertices of the quantum graph  $\Gamma_{60}$ . Note that each vertex is connected to precisely four other vertices, as shown also in Fig. 1, giving rise to the 4-regular (quartic) quantum graph  $\Gamma_{60}$ , illustrated in Fig. 2.

There is an alternative way of rationalizing the above contraction procedure. At the energies we are interested in, one can show that the  $\Gamma_{120}$  wave functions for the energy eigenstates are approximately constant along the flip edges. In this limit, the boundary conditions of  $\Gamma_{120}$  become equivalent to those of  $\Gamma_{60}^\dagger$ . Either way,  $\Gamma_{60}$  only retains edges corresponding to the

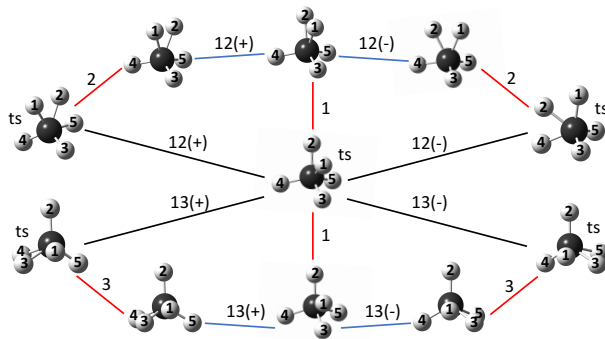


Figure 1: Local structure of the quantum graphs  $\Gamma_{120}$  (blue and red edges) and  $\Gamma_{60}$  (black edges). The red edges correspond to the flip motion and the labels indicate which proton is exchanged from a  $\text{H}_2$  unit to a  $\text{CH}_3^+$  unit. The blue edges correspond to an internal rotation and the labels indicate the  $\text{H}_2$  unit which rotates relative to the  $\text{CH}_3^+$  unit in a clockwise (+) or anticlockwise (-) fashion. The midpoint of each red flip edge is a  $C_{2v}$ -symmetric transition state (ts). In going from  $\Gamma_{120}$  to  $\Gamma_{60}$ , the red edges shrink so that we are left with just the transition states connected by black edges.

internal rotation. Our simplified model therefore has the feature of explaining the low-energy dynamics solely in terms of the internal rotation motion without the flip motion, with the constant wave function argument allowing for backstage full exchange of the protons. This model is thus set up in clear violation of the claim of the authors of Ref. 34, namely that “the combination of the two [internal motions] enables large-amplitude motion and thus ”full scrambling“ ... whereas partial scrambling leads to the well-known small-amplitude motion only”.

We now seek the quantum states corresponding to motion on the  $\Gamma_{60}$  graph. The eigenenergies are found by solving the time-independent Schrödinger equation for a free particle moving along the edges, with the so-called Neumann boundary conditions [31] imposed on the eigenstates. These conditions are that the wave function should be continuous everywhere, with zero total momentum flux out of each vertex. As we have already pointed out,  $\Gamma_{60}$  is a 4-regular graph with all edges having a common length  $l = L_{\text{rot}}$ . Perhaps surprisingly, these properties imply that the structure of the quantum energy levels can be determined entirely from *combinatorial properties* of the graph.

More precisely, given a wave function  $\psi$  defined on the graph  $\Gamma_{60}$  and obeying the time-independent Schrödinger equation along each edge,

$$-\frac{1}{2} \frac{d^2 \psi}{dx^2} = E \psi, \quad (3)$$

where  $x$  is a mass-scaled coordinate, consider the vector of its values at each vertex  $\mathbf{v} = (\psi(v_1), \psi(v_2), \dots)$ . It is straightforward to prove†that  $\psi$  is an eigenfunction with energy  $E$  satisfying the Neumann boundary conditions if and only if

$$\mathbf{A} \mathbf{v} = 4 \cos(\sqrt{2El}) \mathbf{v}, \quad (4)$$

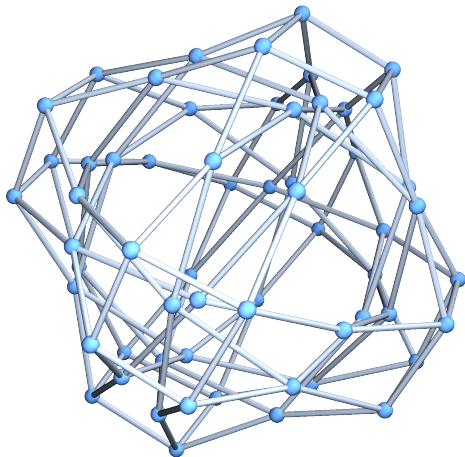


Figure 2: Illustration of the 4-regular quantum graph  $\Gamma_{60}$ . In this model of the quantum dynamics of  $\text{CH}_5^+$  there is a single edge length, connecting versions of  $C_{2v}$ -symmetric transition states, midpoints of the flip edge of  $\Gamma_{120}$ .

*i.e.*, if and only if  $\lambda = 4 \cos\left(\sqrt{2El}\right)$  is an eigenvalue of the *adjacency matrix*  $\mathbf{A}$  for the graph  $\Gamma_{60}$ , with  $\mathbf{v}$  in the corresponding eigenspace.  $\mathbf{A}$  is simply a matrix whose elements indicate whether given pairs of vertices are connected by an edge or not:

$$(A)_{ij} = \begin{cases} 1 & \text{if vertices } v_i, v_j \text{ connected} \\ 0 & \text{otherwise} \end{cases} \quad (5)$$

and is a familiar concept in elementary graph theory [35].

Equation (4) therefore relates the *quantum spectrum* (the eigenvalues of the Hamiltonian) to the so-called *combinatorial spectrum* (the eigenvalues of the adjacency matrix). The combinatorial spectrum is a concept already utilized in molecular spectroscopy [36], and only depends on the connectivity of the graph as encoded in  $\mathbf{A}$ .

To find the combinatorial spectrum of  $\Gamma_{60}$ , we look for roots of the characteristic polynomial  $\chi_{\mathbf{A}}(\lambda) = \det(\lambda\mathbf{I} - \mathbf{A})$  associated with the adjacency matrix  $\mathbf{A}$ . An explicit expression for  $\mathbf{A}$  is easily derived by considering paths of the form illustrated in Fig. 1. In the end, we obtain

$$\chi_{\mathbf{A}}(\lambda) = (\lambda^4 - 9\lambda^2 + 16)^5 (\lambda^4 - 12\lambda^2 + 16)^4 (\lambda^2 - 1)^{11} (\lambda^2 - 16), \quad (6)$$

and the full combinatorial spectrum is given in Table 2. Table 2 also shows the dimensions of the corresponding eigenspaces and the irreps of the MS group  $S_5^*$ .

We pause here to note the striking similarity between Tables 1 and 2. First, note that the combinatorial spectrum splits into positive  $\lambda$  and negative  $\lambda$ , with each corresponding to a total eigenspace dimension of 30. Moreover, the eigenspaces associated with positive  $\lambda$  transform in precisely the same irreps as Block 1 of Table 1, while those associated with negative  $\lambda$  transform precisely like Block 2. Thus, purely combinatorial properties of the quantum graph  $\Gamma_{60}$  have captured the block structure of the lowest vibrational states of  $\text{CH}_5^+$ . Even more interestingly, we have an explanation for the curious relationship between Block 1 states and Block 2 states: this corresponds to a  $\lambda \rightarrow -\lambda$  symmetry of the combinatorial spectrum (see Table 2), under which the  $S_5^*$  irreps are related by multiplication with  $A_2^-$ . The symmetry of the combinatorial

$\lambda$	$\dim(\lambda)$	$S_5^*$ irrep
4	1	$A_1^+$
$1 + \sqrt{5}$	4	$G_2^-$
$\frac{1}{2}(1 + \sqrt{17})$	5	$H_1^+$
$\frac{1}{2}(-1 + \sqrt{17})$	5	$H_2^-$
$-1 + \sqrt{5}$	4	$G_1^+$
1	11	$H_2^+ \oplus I^-$
-1	11	$H_1^- \oplus I^+$
$1 - \sqrt{5}$	4	$G_2^-$
$\frac{1}{2}(1 - \sqrt{17})$	5	$H_1^+$
$\frac{1}{2}(-1 - \sqrt{17})$	5	$H_2^-$
$-1 - \sqrt{5}$	4	$G_1^+$
-4	1	$A_2^-$

Table 2: The combinatorial spectrum of the quantum graph  $\Gamma_{60}$ , where  $\dim(\lambda)$  gives the degeneracy of a given eigenvector corresponding to the eigenvalue  $\lambda$  [see Eq. (6)]

spectrum under  $\lambda \rightarrow -\lambda$  is a simple consequence [35] of the fact that the quantum graph  $\Gamma_{60}$  is *bipartite*: the set of vertices  $V$  can be divided into two disjoint and independent sets  $A$  and  $B$  such that every edge connects a vertex in  $A$  to one in  $B$ . The sets  $A$  and  $B$  are related by odd permutations of the protons<sup>†</sup>.

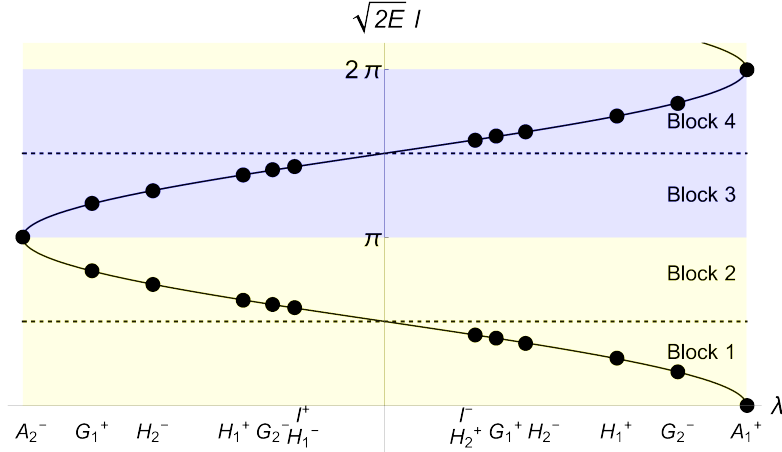


Figure 3: Illustration of the block structure and the symmetry properties of the spectrum of the quantum graph  $\Gamma_{60}$ . Black dots indicate energies of the quantum states.

Equation (4) relates the combinatorial spectrum to the quantum spectrum, as illustrated in Fig. 3. We can see the consequences of the  $\lambda \rightarrow -\lambda$  symmetry for the quantum energy levels: each state in Block 1 comes with a partner in Block 2, with their corresponding values of  $\sqrt{2E}l$  being related by reflection in the line  $\sqrt{2E}l = \pi/2$ . In particular, the dimensionless ratios

$$\frac{\sqrt{E_1(I^-)} + \sqrt{E_2(I^+)}}{\sqrt{E_1(H_1^+) + \sqrt{E_2(H_2^-)}}, \frac{\sqrt{E_1(H_2^+) + \sqrt{E_2(H_1^-)}}}{\sqrt{E_1(H_1^+) + \sqrt{E_2(H_2^-)}}, \dots \quad (7)$$

are all equal to 1 in the  $\Gamma_{60}$  model. This compares very favourably with the variational seven-dimensional model [7, 12, 14] results

$$\frac{\sqrt{E_1(A_1^+)} + \sqrt{E_2(A_2^-)}}{\sqrt{E_1(H_1^+)} + \sqrt{E_2(H_2^-)}} \approx \frac{\sqrt{0} + \sqrt{198}}{\sqrt{20} + \sqrt{139}} \approx 0.86, \quad (8)$$

$$\frac{\sqrt{E_1(G_2^-)} + \sqrt{E_2(G_1^+)}}{\sqrt{E_1(H_1^+)} + \sqrt{E_2(H_2^-)}} \approx \frac{\sqrt{10} + \sqrt{154}}{\sqrt{20} + \sqrt{139}} \approx 0.95, \quad (9)$$

$$\frac{\sqrt{E_1(H_2^-)} + \sqrt{E_2(H_1^+)}}{\sqrt{E_1(H_1^+)} + \sqrt{E_2(H_2^-)}} \approx \frac{\sqrt{41} + \sqrt{122}}{\sqrt{20} + \sqrt{139}} \approx 1.07, \quad (10)$$

$$\frac{\sqrt{E_1(G_1^+)} + \sqrt{E_2(G_2^-)}}{\sqrt{E_1(H_1^+)} + \sqrt{E_2(H_2^-)}} \approx \frac{\sqrt{49} + \sqrt{113}}{\sqrt{20} + \sqrt{139}} \approx 1.08, \quad (11)$$

$$\frac{\sqrt{E_1(I^-)} + \sqrt{E_2(I^+)}}{\sqrt{E_1(H_1^+)} + \sqrt{E_2(H_2^-)}} \approx \frac{\sqrt{58} + \sqrt{112}}{\sqrt{20} + \sqrt{139}} \approx 1.12, \quad (12)$$

and

$$\frac{\sqrt{E_1(H_2^+)} + \sqrt{E_2(H_1^-)}}{\sqrt{E_1(H_1^+)} + \sqrt{E_2(H_2^-)}} \approx \frac{\sqrt{59} + \sqrt{114}}{\sqrt{20} + \sqrt{139}} \approx 1.12. \quad (13)$$

In this paper we have drastically simplified the quantum graph model of the low-energy rovibrational quantum dynamics of  $\text{CH}_5^+$  by reducing the original 120-vertex quantum graph to a 60-vertex graph,  $\Gamma_{60}$ .  $\Gamma_{60}$  was constructed by shrinking the edges corresponding to the flip internal motion that exchanges a pair of protons between the  $\text{H}_2$  and  $\text{CH}_3^+$  units of the equilibrium structure of  $\text{CH}_5^+$ . Thus, at first sight we neglect one of the two important large-amplitude internal motions characterizing the exchange dynamics (scrambling) of the H atoms of  $\text{CH}_5^+$ . This allows us to obtain the quantum states of  $\Gamma_{60}$  in analytic form, with the structure of the energy levels depending only on combinatorial properties. The eigenvalues of this simple 1D, potential-free model are in excellent agreement with the first 60 vibrational states determined by sophisticated variational nuclear-motion computations utilizing a potential energy hypersurface. Furthermore, the bipartite structure of  $\Gamma_{60}$  gives a natural explanation for symmetries in the vibrational energy level structure of  $\text{CH}_5^+$ , again in perfect agreement with the results of variational nuclear dynamics computations. Note that neither the variational computations [7, 12, 14] nor the quantum-graph models [15, 27] yield only the Pauli-allowed states of  $\text{CH}_5^+$  (states with  $A_2^\pm$ ,  $G_2^\pm$ , and  $H_2^\pm$  symmetry have non-zero spin-statistical weights), so our discussion focused on *all* possible states; the non-existing states can be filtered out *a posteriori*.

## Acknowledgements

The work of JIR was supported by the EPSRC grant CHAMPS EP/P021123/1. The work performed in Budapest received support from NKFIH (grant no. K119658) and from the ELTE Institutional Excellence Program (TKP2020-IKA-05) financed by the Hungarian Ministry of Human Capacities.

## References

- [1] George A. Olah and Richard H. Schlosberg. Chemistry in super acids. i. hydrogen exchange and polycondensation of methane and alkanes in  $\text{fso}_3\text{h-sbf}_5$  ("magic acid") solution. protonation of alkanes and the intermediacy of  $\text{ch}_5^+$  and related hydrocarbon ions. the high chemical reactivity of "paraffins" in ionic solution reactions. *J. Am. Chem. Soc.*, 90(10):2726–2727, 1968.
- [2] George A. Olah, Gilles Klopman, and Richard H. Schlosberg. Super acids. iii. protonation of alkanes and intermediacy of alkanonium ions, pentacoordinated carbon cations of  $\text{ch}_5^+$  type. hydrogen exchange, protolytic cleavage, hydrogen abstraction; polycondensation of methane, ethane, 2,2-dimethylpropane and 2,2,3,3-tetramethylbutane in  $\text{fso}_3\text{h-sbf}_5$ . *J. Am. Chem. Soc.*, 91(12):3261–3268, 1969.
- [3] G. A. Olah. *Carbocations and Electrophilic Reactions*. VCH-Wiley Publishers, Weinheim, 1974.
- [4] G. A. Olah. *My Search for Carbocations and Their Role in Chemistry*, pages 149–176. December 1994.
- [5] Edmund T. White, Jiang Tang, and Takeshi Oka.  $\text{CH}_5^+$ : the infrared spectrum observed. *Science*, 284:135–137, 1999.
- [6] Oskar Asvany, Padmanabhan Padma Kumar, Britta Redlich, Ilka Hegemann, Stephan Schlemmer, and Dominik Marx. Understanding the infrared spectrum of bare  $\text{ch}_5^+$ . *Science*, 309(5738):1219–1222, 2005.
- [7] X.-G. Wang and T. Carrington Jr. Vibrational energy levels of  $\text{CH}_5^+$ . *J. Chem. Phys.*, 129:234102, 2008.
- [8] Sergei D. Ivanov, Oskar Asvany, Alexander Witt, Edouard Hugo, Gerald Mathias, Britta Redlich, Dominik Marx, and Stephan Schlemmer. Quantum-induced symmetry breaking explains infrared spectra of  $\text{CH}_5^+$  isotopologues. *Nat. Chem.*, 2:298–302, 2010.
- [9] Oskar Asvany, Koichi M. T. Yamada, Sandra Brünken, Alexey Potapov, and Stephan Schlemmer. Experimental ground-state combination differences of  $\text{CH}_5^+$ . *Science*, 347:1346–1349, 2015.
- [10] Robert Wodraszka and Uwe Manthe.  $\text{Ch}_5^+$ : Symmetry and the entangled rovibrational quantum states of a fluxional molecule. *J. Phys. Chem. Lett.*, 6(21):4229–4232, 2015.



- [11] Hanno Schmiedt, Stephan Schlemmer, and Per Jensen. Symmetry of extremely floppy molecules: Molecular states beyond rotation-vibration separation. *J. Chem. Phys.*, 143(15):154302, 2015.
- [12] Xiao-Gang Wang and Tucker Carrington. Calculated rotation-bending energy levels of  $\text{ch}_5^+$  and a comparison with experiment. *J. Chem. Phys.*, 144(20):204304, 2016.
- [13] Stefan Brackertz, Stephan Schlemmer, and Oskar Asvany. Searching for new symmetry species of  $\text{ch}_5^+$  – from lines to states without a model. *J. Mol. Spectrosc.*, 342(Supplement C):73 – 82, 2017.
- [14] C. Fábri, M. Quack, and A. G. Császár. On the use of nonrigid-molecular symmetry in nuclear-motion computations employing a discrete variable representation: a case study of the bending energy levels of  $\text{CH}_5^+$ . *J. Chem. Phys.*, 147:134101, 2017.
- [15] C. Fábri and A. G. Császár. Vibrational quantum graphs and their application to the quantum dynamics of  $\text{CH}_5^+$ . *Phys. Chem. Chem. Phys.*, 20:16913–16917, 2018.
- [16] Attila G. Császár, Csaba Fábri, and János Sarka. Quasistructural molecules. *WIREs Comput. Mol. Sci.*, 10(1):e1432, 2020.
- [17] Grigory A. Natanson, Gregory S. Ezra, Gerardo Delgado-Barrio, and R. Stephen Berry. Calculation of rovibrational spectra of water by means of particles-on-concentric-spheres models. i. ground stretching vibrational state. *J. Chem. Phys.*, 81(8):3400–3406, 1984.
- [18] Grigory A. Natanson, Gregory S. Ezra, Gerardo Delgado-Barrio, and R. Stephen Berry. Calculation of rovibrational spectra of water by means of particles-on-concentric-spheres models. ii. excited states of stretching vibrations. *J. Chem. Phys.*, 84(4):2035–2044, 1986.
- [19] David M. Leitner, Grigory A. Natanson, R. Stephen Berry, Pablo Villarreal, and Gerardo Delgado-Barrio. Particles-on-a-sphere method for computing the rotational-vibrational spectrum of  $\text{h}_2\text{o}$ . *Comput. Phys. Commun.*, 51(1):207 – 216, 1988.
- [20] John E. Hunter, David M. Leitner, Grigory A. Natanson, and R. Stephen Berry. Theoretical intensities for rotation-vibration lines of water using particles-on-a-sphere wavefunctions. *Chem. Phys. Lett.*, 144(2):145 – 148, 1988.
- [21] Michael P. Deskevich and David J. Nesbitt. Large amplitude quantum mechanics in polyatomic hydrides. i. a particles-on-a-sphere model for  $\text{xh}_n$ . *J. Chem. Phys.*, 123(8):084304, 2005.
- [22] Michael P. Deskevich, Anne B. McCoy, Jeremy M. Hutson, and David J. Nesbitt. Large-amplitude quantum mechanics in polyatomic hydrides. II. A particle-on-a-sphere model for  $\text{XH}_n$  ( $n = 4, 5$ ). *J. Chem. Phys.*, 128:094306, 2008.
- [23] Felix Uhl, Łukasz Walewski, Harald Forbert, and Dominik Marx. Adding flexibility to the “particles-on-a-sphere” model for large-amplitude motion: Posflex force field for protonated methane. *J. Chem. Phys.*, 141(10):104110, 2014.

- [24] H. Schmiedt, P. Jensen, and S. Schlemmer. Collective molecular superrotation: A model for extremely flexible molecules applied to protonated methane. *Phys. Rev. Lett.*, 117:223002, 2016.
- [25] Hanno Schmiedt, Per Jensen, and Stephan Schlemmer. Rotation-vibration motion of extremely flexible molecules – the molecular superrotor. *Chem. Phys. Lett.*, 672(Supplement C):34 – 46, 2017.
- [26] Hanno Schmiedt, Per Jensen, and Stephan Schlemmer. The role of angular momentum in the superrotor theory for rovibrational motion of extremely flexible molecules. *J. Mol. Spectrosc.*, 342(Supplement C):132 – 137, 2017.
- [27] J. I. Rawlinson. Quantum graph model for rovibrational states of protonated methane. *J. Chem. Phys.*, 151(16):164303, 2019.
- [28] Linus Pauling. The diamagnetic anisotropy of aromatic molecules. *J. Chem. Phys.*, 4(10):673–677, 1936.
- [29] J. I. Rawlinson. An alpha particle model for carbon-12. *Nucl. Phys. A*, 975:122 – 135, 2018.
- [30] J. I. Rawlinson. *Rovibrational Dynamics of Nuclei and Molecules*. PhD thesis, University of Cambridge, 2020.
- [31] Gregory Berkolaiko and Peter Kuchment. *Introduction to Quantum Graphs*, volume 186. American Mathematical Society, 2013.
- [32] P. R. Bunker and P. Jensen. *Molecular symmetry and spectroscopy*. NRC Research Press, Ottawa, 2006.
- [33] Peter R. Schreiner, Seung-Joon Kim, Henry F. Schaefer III, and Paul von Ragué Schleyer.  $\text{CH}_5^+$ : The never-ending story or the final word? *J. Chem. Phys.*, 99(5):3716–3720, 1993.
- [34] Alexander Witt, Sergei D. Ivanov, and Dominik Marx. Microsolvation-induced quantum localization in protonated methane. *Phys. Rev. Lett.*, 110:083003, 2013.
- [35] N. Biggs. *Algebraic Graph Theory*. Cambridge University Press, 1993.
- [36] P. Árendás, T. Furtenbacher, and A. G. Császár. On spectra of spectra. *J. Math. Chem.*, 54:806–822, 2016.